

Saturn's Hydrogen Aurora as Observed by HST

John Trauger, JPL
John Clarke, U of Michigan
Gilda Ballester, U of Michigan
Lotfi Ben Jaffel, IAP
Karl Stapelfeldt, JPL
Robin Evans, JPL

Poster presentation to the Conference on the
Magnetospheres of the Outer Planets

Paris, France
9-14 August 1999

Overview

We describe Saturn's aurora as observed by HST in 10/1994, 10/1995, and 10-12/1997. HST provides access to the auroral emissions due to atomic and molecular hydrogen in the northern and southern auroral zones. Also seen are the dark stratospheric polar caps produced by the aurora, and the FUV appearance of Saturn's rings, which show diurnal variations in Ly α emission. These observations were taken with WFPC2 during 1994-5, and more recently with STIS using both the FUV imaging and spectroscopic modes. Thus far, twelve HST observing orbits have provided a sparsely sampled timeline of Saturn's auroral activity. An additional eight HST orbits of STIS imaging and spectroscopy are scheduled in late 1999.

In 1997, molecular hydrogen auroral emissions (1350-1800Å) were consistently seen to be tightly confined at latitudes near 72-75° in the south at dawn, wandering to higher latitudes with generally more complex and variable morphology by dusk. Auroral Ly α emissions are consistently more diffuse, extending $\sim 1^\circ$ north and south of the molecular emission latitudes. Auroral arcs seen in the north during the 1994-5 apparitions were confined near 76° latitude at dawn, also moving higher towards dusk. The auroral arcs have a persistent morphology that is roughly fixed in local time, but with slow (hours) variations in the mean latitudes of the auroral emissions and often rapid (minutes) variations in locally bright emission features. The STIS imaging data have been taken in time-tagged mode, providing further insight into the variables of the auroral emissions during the period of observations. The observed auroral features have been modeled to unfold the latitude, longitude, vertical extent, and radiated power of the emissions. The radiated power in the aurora has been seen to vary from unobservable to 4×10^{10} watts with peak surface brightness up to 90 kRay in the 1994-5 WFPC2 images. This range brackets the $1-2 \times 10^{10}$ watts and 20-30 kRay peak surface brightnesses that were observed with STIS in 1997. The 1999 STIS observations are designed to provide, for the first time, HST imaging and spectroscopy over a full rotation of the planet in order to capture a complete picture of the south auroral emission region on Saturn. A complete rotation is required to sort out the planet-fixed and local-time-fixed characteristics, and to provide spectra with sufficient S/N to usefully constrain models of the FUV aurora and NUV atmospheric radiative transfer.

HST Observations of Saturn's Aurora

The Saturn aurora was first observed with HST/FOC on 2 October 1994 (Gérard *et al.* 1995). Eight individual exposures (8400 seconds in total), covering a 13-hour observing period with FOC's F152M+F175W filter combination, were coadded to produce an auroral detection. About seven auroral brightenings were reported near 80° north latitude. The long exposure precludes further information on the time development or movement of the features.

HST/WFPC2 imaging of Saturn's aurora was obtained in October 1994 and 1995 with far-ultraviolet (FUV) filter combinations that include the emission lines of H₂ (Lyman and Werner bands shortward of 1650Å), atomic hydrogen Ly α , and the Rayleigh-scattered solar continuum longward of 1700Å (Trauger *et al.* 1998a). A physical model was used to unfold the planetocentric distribution of the aurora from the images. Auroral intensities were computed for each image in terms of a large number of individual bundles of magnetic field lines (Connerney *et al.* 1983) illuminated with a Chapman profile, each originating from a grid of "footprints" on the reference 1-bar surface. These individual model components are each convolved with a representative HST point spread function. The distribution of auroral emissions was determined by least-squares fitting of the projected intensities of these individual model components to the data. This unfolds the three-dimensional distribution of the auroral emissions in terms of a physically meaningful vertical profile. Peak auroral surface brightnesses observed for Saturn reached ~ 90 kR and an integration of the northern auroral emissions yielded a total FUV radiated power as large as $\sim 4 \times 10^{10}$ Watts. The intensities of the observed aurorae showed significant variability on the time scales of 1000 seconds or less. The location of the brightest emissions appeared generally stationary in local time, suggesting an excitation mechanism that is dominated by interactions between the solar wind and planetary magnetosphere.

HST/STIS observations of Saturn's aurora were carried out in October 1997 (Trauger *et al.* 1998b) using both the imaging and spectroscopic modes, providing access to the auroral emissions from atomic and molecular hydrogen in the northern and southern auroral zones. As seen in Figures 2a-2e, STIS

imaging with and without the SrF₂ blocker provided discrimination between hydrogen Ly α and H₂ emissions in the 1200-1650Å wavelength range (Figure 1a and 1b). Both atomic and molecular emissions are seen in the STIS clear imaging mode, while the addition of the SrF₂ longpass filter discriminates against Ly α to isolate the H₂ molecular emissions. Time-tagged imaging provided the movements of auroral emissions on 100-second time scales, while summation provided the greatest S/N for persistent features. These images extend the WFPC2 observations with improved sensitivity and spectral discrimination. As for the WFPC2 data, the observed auroral features have been modeled to unfold the latitude, longitude, vertical extent, and radiated power of the emissions. These observations also show a persistent arc morphology that is roughly fixed in local time, and with slow movement in the mean latitudes of the auroral arcs and in locally-bright emission features within the arcs themselves.

The difference image in Figure 1c illustrates how the optically-thick Ly α emission is distributed over the disk. It decreases gradually in intensity toward the limb, then increases sharply to a maximum at the limb just above the homopause due to increased scattering in the wings of the line (*Gladstone 1995*). This emission is blocked by the rings passing in front of Saturn, and not blocked by the rings passing behind the planet. The vertical profile of the H Ly α emission is made apparent by azimuthally summing the vertical profiles along the limb, providing the extent and temperature of the highest altitude portion of Saturn's atmosphere. The observed altitude of peak emission also correlates with the location of the homopause, for comparison with the altitude distribution of the auroral emissions.

The Ring Atmosphere

The appearance of the rings in H Ly α reveals more detail than expected. From local morning, on the left, the rings begin much darker than the interplanetary sky background emission, gradually brightening with local time until they are much brighter than the sky background before disappearing behind Saturn's limb. This suggests that a solar radiation is driving a production process that releases H atoms into the ring's atmosphere. This in turn is suggestive of "photo-sputtering" (Carlson 1980), in which solar EUV flux was proposed to release H atoms from the water ice surface. The local time dependence is also reminiscent of the action of the ring "spokes" found in Voyager images (Goertz 1983), believed to be caused by levitated dust. Finally, the appearance of apparent brightening in H Ly α in the Cassini division and the outer edge of the visible rings suggest more complicated processes leading to localized enhancements of the atomic hydrogen "atmosphere" of the rings.

Polar Hazes

Saturn's aurora has been associated with dark polar absorption caps, seen with greatest contrast at shorter UV wavelengths, and also with less contrast in the visible (*West et al. 1983; Pryor and Hord 1991; Karkoschka and Tomasko 1993; Ben Jaffel et al. 1995; Gérard et al. 1995*). The dark polar caps are attributed to stratospheric aerosols produced above the 10 mBar level that are distinctly smaller ($\sim 0.15\mu\text{m}$) than typical tropospheric aerosols ($\sim 1.5\mu\text{m}$), and may be produced directly from the stratospheric gases (*Karkoschka and Tomasko 1993*). Several paths to the formation of the polar haze have been suggested. Production by auroral-driven ion chemistry has been outlined by Strobel (*1983, 1985*). The main reactions are electron-impact ionization of H_2 , followed by the production of H_3^+ , which quickly reacts with CH_4 to form CH_5^+ , leading to further subsequent reactions with other hydrocarbons and/or the dissociative recombination to form radicals, all driving further chemical reactions to form larger haze molecules. Other proposed paths of haze formation include the photochemical processing of CH_4 (*Gladstone 1983*) and auroral heating that affects the chemistry and dynamics of the local atmosphere (*Pryor and Hord 1991*).

The ultraviolet reflectivity of the outer planets can provide information about the chemical composition in the stratosphere and the upper troposphere. Even as trace species, the absorption signatures of hydrocarbons and complex molecules dominate the 1200-1700Å range, providing an efficient means to derive their abundances and vertical distribution. A solar reflection spectrum with superimposed absorption bands of trace gases and aerosols is seen longward of 1700Å. While imaging reveals large scale patterns of the stratospheric and upper tropospheric morphology versus latitude and longitude, the analysis of reflected spectra from localized regions provides the vertical structure. Rayleigh scattering by H_2 , molecular absorption by H_2 , C_4H_2 , C_2H_4 , CH_4 , C_2H_2 , C_2H_6 , H_2O , AsH_3 , PH_3 , CO_2 , GeH_4 and NH_3 , and absorbing/scattering aerosols are all seen in the FUV/NUV spectra (*Ben Jaffel et al. 1995*). An IUE spectrum of Saturn running from 1400 to 3000Å, representing an average over the full Saturn disk, has been analyzed (*Ben Jaffel et al. 1998*). The IUE spectrum is dominated by the low latitude non-auroral regions, in which aerosols near the tropopause do not strongly affect the altitude range probed by ultraviolet.

let wavelengths in the model. However, polar hazes are significant at the auroral latitudes, and this means that FUV/NUV spectra with sufficient spatial resolution and S/N could discern the latitude dependence and onset of the hazes at high latitudes. STIS spectra will be obtained in late 1999, to determine the characteristics (particle size, etc.) and the vertical structure of the polar haze as a function of latitude.



Figure 1. **Saturn's FUV Aurora.** From left to right, the panels show the appearance of Saturn in the (a) STIS 25MAMA clear imaging mode, (b) in the F25SRF2 mode with an SrF_2 filter blocking wavelengths shortward of 1350\AA to distinguish the atomic and molecular emissions, and (c) the difference of these two images, showing the $\text{H Ly}\alpha$ features of the aurora, disk, and rings. Images (a) and (b) are respectively the summations of the right and left images in Figures 2a-2d.

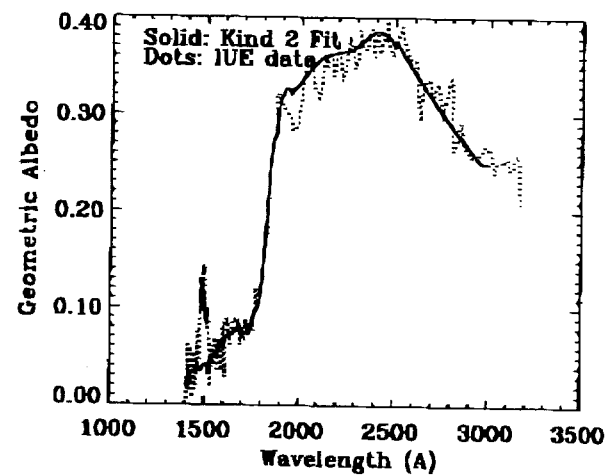
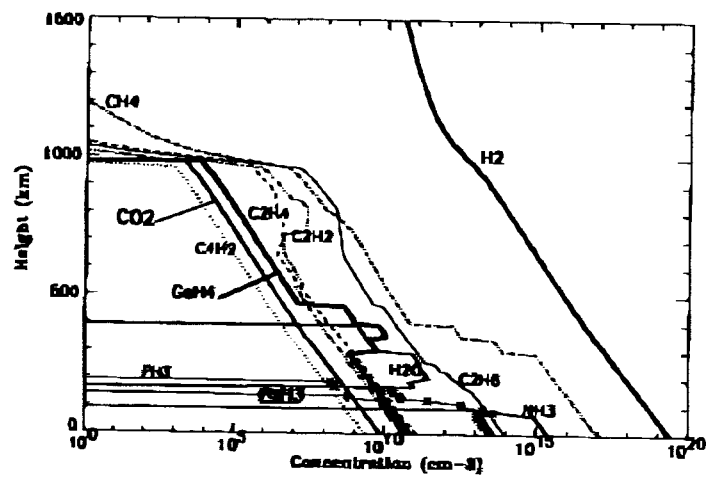


Figure 3. Trace gas absorption in the FUV and NUV. Density profiles appearing at left were determined by fitting an IUE spectrum of Saturn's disk, shown at right, with a radiative transfer model for UV-absorbing gases. Spatial discrimination between the polar and lower latitude areas will be improved with STIS spectra scheduled later this year.

References

- Ballester, G.E., et al., *Science* 274, 409, 1996.
- Ben Jaffel, L., V. Leers, and B.R. Sandel, *Science* 269, 951, 1995.
- Ben Jaffel, L. et al., *BAAS* 30, 1096, 1998.
- Carlson, R.W., *Nature* 283, 461, 1980.
- Clarke, J.T., et al., *Science* 274, 404, 1996.
- Connerney, J.E.P., et al., *J. Geophys. Res.* 88, 8779, 1983.
- Gérard, J.-C. et al., *J. Geophys. Res.* 22, 2685, 1995.
- Gladstone, G.R., *Ph.D. Thesis, Caltech*, 1983.
- Karkoschka, E. and M.G. Tomasko, *Icarus* 106, 428, 1993.
- Pryor, W.R. and C.W. Hord, *Icarus* 91, 161, 1991.
- Strobel, D.F., *Int. Rev. Phys. Chem.* 3, 145, 1983.
- Strobel, D.F., *The Photochemistry of Atmospheres, Levine ed.* , 393, 1985.
- Trauger, J., et al., *J. Geophys. Res.* 103, 20237, 1998a.
- Trauger, J., et al., *BAAS* 29, 1255 and *BAAS*, (DPS meeting), 1998b.
- West, R.A., et al., *J. Geophys. Res.* 88, 8679, 1983.